

# Linear microfocus bremsstrahlung generated in light and heavy narrow targets in B-18 betatron

M M Rychkov, V V Kaplin, E L Malikov, V A Smolyanskiy, I B Stepanov,  
A S Lutsenko, V Gentsel'man and I K Vas'kovskii

National Research Tomsk Polytechnic University, P.O. Box 25, 32 Lenin Ave. ,  
634050 Tomsk, Russia

E-mail: rychkov@tpu.ru

**Abstract.** The first results of studying the properties of X- and G-ray beams generated at the grazing incidence of 18-MeV electrons with the 50 and 8- $\mu\text{m}$ -thick Si crystals and a 13- $\mu\text{m}$ -thick Ta foil of 4 mm in length along the electron beam are presented. The target has been placed in a goniometer inside the chamber of a B-18 betatron. The results exhibit strong changes in the angular distribution of radiation at the variation of the orientation of the target. This effect is not observed in the case of the normal incidence of electrons on the surface of a thin target. Images of a reference microstructure have been obtained with a high resolution of details of the microstructure owing to the smallness of the source of radiation. The dependence of the contrast of an image on the position of the microstructure in the radiation cone has been demonstrated, which is determined by the change in the effective size of the radiation source when the emission angle of the source is changed.

## 1. Introduction

The production of a microfocus radiation source based on relativistic electron beams is an important part of accelerator physics. For low-energy electrons, for example, in X-ray tubes, this problem was solved by sharp focusing of the electron beam on the target to obtain a focal spot with a diameter in the micron region. For linear electron accelerators, this method is applicable, but not effective enough. In the case of cyclic accelerators, the method of focusing an electron beam is not applicable. But, in [1, 2] the idea was proposed to use internal targets with a much smaller diameter of the beam of accelerator electrons in the cyclic accelerator to reduce the focal spot of the generated Bremsstrahlung (Bs). Here, if the beam circulates for a sufficiently long time on the radius of the micro-target location, then, due to betatron oscillations, electrons will fall on such a target with a sufficiently high efficiency. Later, this effect was realized on a miniature synchrotron [3].

Betatrions generating secondary hard radiation caused by interaction of the internal electron beam with the target (typically a thick target) that is larger in its area than the cross section of the millimeter-sized beam are used for obtaining the images of a number of objects. This paper presents the results obtained for generation of linear microfocal bremsstrahlung (LMBs) under interaction of 18 MeV electrons with thin targets which were oriented along the direction of the internal beam of the B-18 betatron in order that the electrons can interact with the narrow front face of the target. Magnified images of the standard microstructure have been obtained using the radiations generated in the three narrow internal targets, the width of the thinnest one is approximately 190 times smaller than the



diameter of the electron beam. The formation of microstructure images with participation of a phase-contrast effect is shown for the first time in the case of a betatron. It was shown also that the image contrast depends on the position of the microstructure in the radiation cone.

## 2. Experimental setup

The experimental conditions shown in Figure 1 were similar to those reported in previous study [4]. A thin experimental target was placed on a thin vertical goniometer holder inside the equilibrium orbit of the accelerated electrons, Figure 1a.

Additional magnetic field generated by the dump coil within 30  $\mu$ s reduced the orbit radius and the electrons fell onto the target oriented along the direction of the beam with a frequency of 50 Hz. The generated radiation escaped through the 50  $\mu$ m Mylar window of the experimental chamber and fell on the Kodak X-ray film placed at a distance of 56 cm from the target. For further analysis, the photographs of the radiation beams were processed with the scanner.

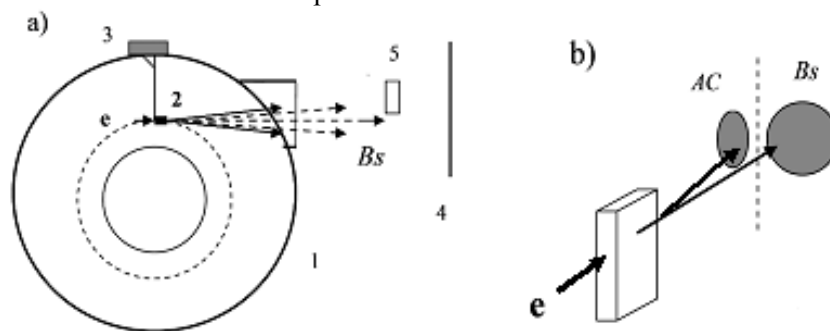


**Figure 1.** The experimental scheme: a) 1 – betatron chamber, 2 – thin target, 3 – goniometer, Bs – Bremsstrahlung, 4 – X-ray film, 5 – microstructure; b) Location of thin target on the electron beam.

The vertical dashed line indicates the target plane direction. AC – Additional Bs Components.

Figure 1b shows the disposition of thin target relative to the direction of the electron beam falling on the front narrow face of the wafer. The goniometer allows to rotate the target about its vertical axis so that the electrons could fall on one or the other lateral surface of the target. The angle of the crystal orientation relative to the electron beam direction could be changed within  $5^\circ > \theta_0 > -5^\circ$ . The region of negative angles  $\theta_0$  corresponded to the electron beam incidence on the target surface turned towards the accelerator center. The 50 and 8- $\mu$ m-thick Si crystals and a 13- $\mu$ m-thick Ta foil with the vertical  $L = 5$  mm and horizontal  $T = 4$  mm (along the direction of the electron beam) sizes were used in the experiments.

The size of the radiation source focus was measured with the *Duplex IQI EN462-5/ASTM E2002-98* microstructural device (*Computerised Information Technology Ltd.*) [5]. The device was installed at a distance of 38 cm from the crystal and could be moved relative to the beam axis to produce the X-ray pattern (negative image) of its components in different areas of the radiation cone. The X-ray patterns were recorded using the X-ray films installed at a distance of 114 cm from the crystal. The X-ray patterns were processed with the scanner to obtain positive images of the device structure and densitograms of these images for subsequent analysis.

## 3. Angular distributions of X-rays

The experiment has shown that the angular distribution of radiation varied depending on the inclination angle  $\theta_0$  of the target. Figure 2 shows the photographs of the angular distributions of the radiations generated by 18 MeV electrons in the 50  $\mu$ m Si wafer oriented at angles  $\theta_0 = 1.9^\circ$  and  $0.05^\circ$  with respect to the electron beam, photographs 1–2, respectively. The images on the X-ray film were formed mainly by X-rays with photon energy in the range of 5 – 50 keV. The densitograms measured

along the horizontal lines passing through the centers of the blackening spots in the angular distribution photographs are provided below.

Photograph 1 shows a blackening spot oriented along the direction of the electron beam and a bright line oriented along the wafer plane direction formed by radiation absorption in the wafer and additional refraction of the radiation portions passing through the wafer lateral surfaces, which appear if the angular distance between the electron beam and the wafer plane direction is sufficiently large. At crystal orientation  $\theta_0 = 0.05^\circ$  along the direction of the electron beam, the angular

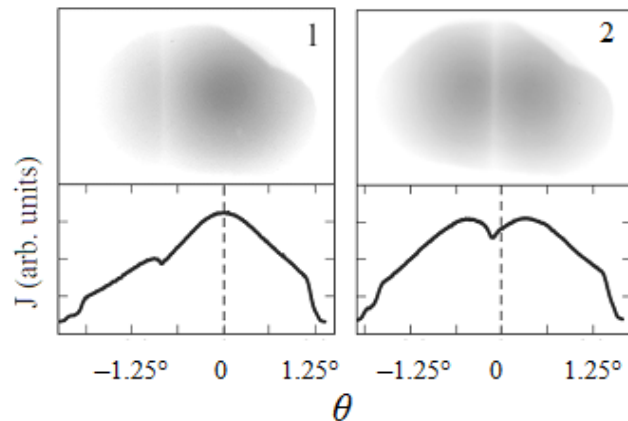


**Figure 2.** Photographs of angular distributions of X-rays at 50  $\mu\text{m}$  Si target orientations  $\theta_0 = 1.9^\circ$  and  $0.05^\circ$ , 1 and 2, respectively. Densitograms are given below.

distribution consists of two broad intensity spots on both sides of the bright line in the direction of the wafer projection, which are formed by two bremsstrahlung radiation beams generated by two portion of electrons into which the original beam is divided during its interaction with the crystal.

In the case of the 8  $\mu\text{m}$  Si wafer the behavior of the radiation distribution at changing the wafer orientation is similar to the above described one.

Figure 3 shows the photograph of angular distribution of the radiation generated by 18 MeV electrons in the 13  $\mu\text{m}$  Ta foil oriented at angle  $\theta_0 = -0.3^\circ$  with respect to the electron beam.

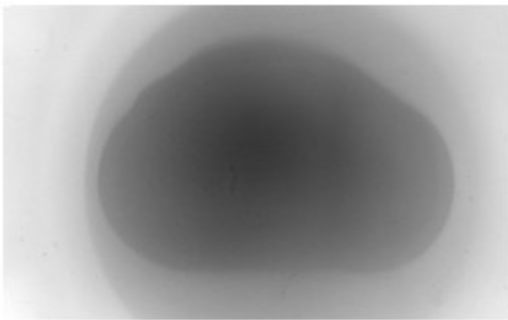


**Figure 3.** Photographs of angular distribution of X-rays at 13  $\mu\text{m}$  Ta target orientation  $\theta_0 = -0.3^\circ$  with respect to the direction of electron beam.

The angular distribution differs significantly from the distributions obtained using the Si crystals. Here, the radiation photograph is formed by harder radiation, since the softer part of the generated spectrum is suppressed by absorption in the heavier target material. This is evidenced by the presence on the photo of images of the flange details of the exit window of the betatron chamber, which were not detected using the softer photons generated in the Si plate, because of their less penetrating power.

#### 4. The *Duplex IQI* images with participation of the effect of edge phase contrast

The generated radiation beams were used to obtain images of the reference microstructure *Duplex IQI*, which indicates high resolution of its components due to a small horizontal size of the radiation source with the widths of about 30, 190 (Si) and 115 (Ta) times smaller than the diameter of the electron beam. The images of the reference microstructure give possibility to evaluate the quality of X-ray

patterns and to estimate the size of a source. The X-ray pattern quality is determined by the number of the detected components of the device, which consists of 13 wire pairs embedded in the plastic holder 4 mm thick and  $15 \times 70 \text{ mm}^2$  in size. The gaps between Pt or W wires with diameters varying from pair to pair within the range of 0.8 – 0.05 mm are equal to the diameter of the wires of a particular pair. The X-ray pattern quality depends on the number of wire pairs, the gaps of which can be identified in the image. The increased size of the radiation source leads to the increased number of wire pairs merged into a single image. The method [6] was developed to evaluate the size of the used radiation source through the darkening profile parameters on the X-ray pattern of the pair, which image almost merges into a single image.

Figure 4 shows a X-ray pattern (1) and positive image (2) of the fragments of the *Duplex IQI*, which were obtained by processing of the X-ray patterns measured with a threefold magnification at the 50  $\mu\text{m}$  Si wafer orientation  $\theta_o = 0.05^\circ$  ( photograph 2, Figure 2).

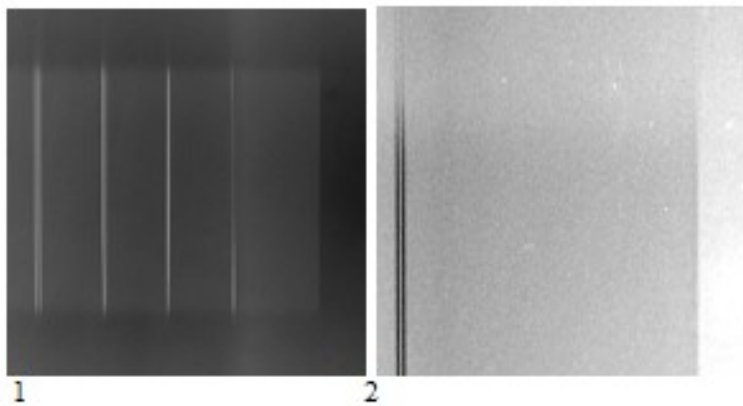


**Figure 4.** X-ray pattern and positive image of Duplex IQI.

With our radiation source geometry in the form of a narrow vertical line, the device *IQI* plane was normal to the cone axis during measurements, and the wire pairs were placed parallel to the crystal plane to achieve their best resolution. Therefore, the wire pair images were parallel to a bright line on the X-ray pattern presented in Figure 2. Note that the image contrast of the device right edge is high and the images of the device upper and lower edges are blurred due to a large vertical size of the radiation source.

Photograph 2 in Figure 4 shows the image obtained by additional magnification of the fragment of the image of the *Duplex IQI* in order to demonstrate a magnified image of the *IQI* device angle. The photograph 2 demonstrates very high contrast in the image of the details of the 13<sup>th</sup> pair. It is also clearly seen that the image of the right edge is made up of dark and bright narrow lines that enhance the contrast of right edge image. That is typical manifestation of the phase contrast at the abrupt interface between two media with different dielectric permittivity [7].

Using the X-ray beam generated in the 8  $\mu\text{m}$  Si target the image of the *Duplex IQI* obtained has higher contrast of its elements than that obtained using the 50  $\mu\text{m}$  Si internal target. Here, clearer phase-contrast in the image of the right edge of *IQI* was observed. The edge images obtained at the 50 and 8  $\mu\text{m}$  Si targets are shown in Figure 5.

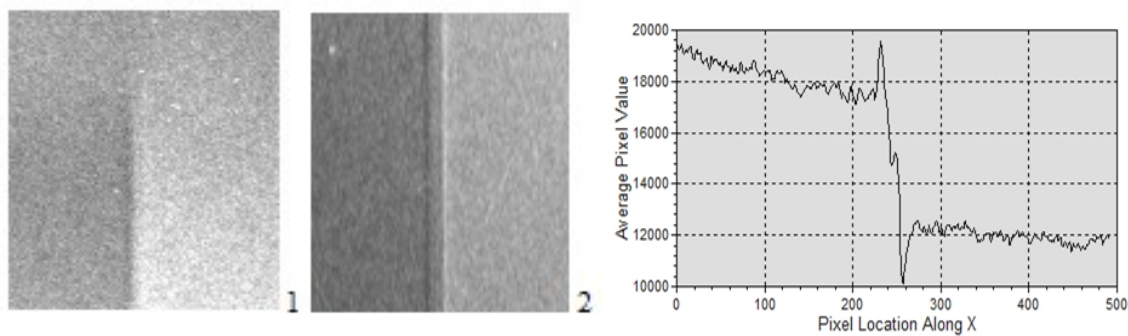


**Figure 5.** The positive images 1 and 2 of the edge of the *Duplex IQI* obtained using the X-ray beams generated in the 50 and 8  $\mu\text{m}$  Si wafers, respectively. The densitogram – for the image 2.

One can see that the edge image 2 has more fine structure consisted of the dark and bright lines much more narrow than that observed at the 50  $\mu\text{m}$  Si target, image 1. The image 2 densitogram demonstrates sharp maximum and minimum of blackening on the photograph 2 along a line perpendicular to the edge.

Figure 6 (1) shows the image of an assembly of four steel plates with the thicknesses of 15, 10, 15 and 15 mm that was obtained with a magnification of 2.4 using a hard bremsstrahlung (photon energy  $> 1$  MeV) generated in the 13 m Ta target. The plates with different rectangular forms were arranged one after another so that the radiation passed through different steel thicknesses in different parts of the assembly. These parts are marked in Figure 6 (1) with markers 1-4. The side face of right edge (near markers 1 and 3) of the first plate 15 mm thick was oriented along the direction of the gamma rays which hit this edge of the plate. Gamma rays passed through the steel plates with total thicknesses of 35, 25, 45 and 40 mm in the regions near the markers 1-4, respectively. The second plate 10 mm thick was placed behind the first plate. The side face of this plate was parallel to the first plate one.

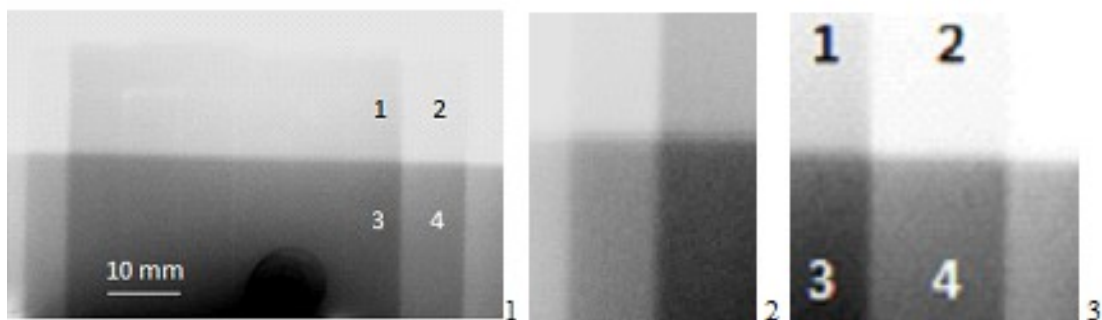


**Figure 6.** The image with a magnification of 2.4 of an assembly of four steel plates obtained using a hard bremsstrahlung beam, Figure 3, generated in the 13 m Ta target.

Figure 6 (1) demonstrates the increased contrast of the images of the right side faces of these plates near markers 1-4. This is due to the phase contrast effect, since the source size in this case is about 13  $\mu\text{m}$ . The images of the left faces of the plates are blurred. Images of these faces are formed by the portion of radiation emitted from the target at an angle of about  $4^\circ$  with respect to the surface of the target. Probably, in this case the phase contrast effect is not realized because of a sufficiently large effective size of radiation source. In this case the absorption contrast forms mainly the edge images of plates. Additionally increased images of left and right edges of the steel plates are shown for comparison in Figures 6 (2) and 6 (3), respectively. The dependence of the effective size of the source

extended along electron beam, from the object position in the radiation cone is discussed in the next section of the article.

### 5. The dependence of image contrast from *Duplex IQI* position in radiation cone

In our case of the radiation source extended along the electron beam, the image contrast of a certain wire pair depends on the source projection along the direction of this pair. When orienting the 50  $\mu\text{m}$  Si wafer along the direction of the electron beam (Figure 2–2), the resolution of the microstructure components located near the plane direction of the wafer (a bright line in Figure 2–2) is expected to be high. In our case of small horizontal angles  $\theta_H$  of the radiation emission from the wafer, the effective horizontal size of the radiation as  $S_H = t + T \cdot |\theta_H|$ . The effective vertical size of the source  $S_V = d \cdot \cos \theta_V$  can be evaluated electron beam diameter  $d$  and does not significantly depend on the vertical angular position  $\theta_V$  of the observation point in the radiation cone as the radiation cone is about  $3^\circ$ . Due to the dependence of  $S_H$  on  $\theta_H$ , the *IQI* device images were obtained for various positions of the device in the radiation cone. The images of the 13th pair of the *IQI* device were analyzed. This pair is used to indicate the best image quality; it consists of a pair of platinum wires of 50  $\mu\text{m}$  in diameter with a 50  $\mu\text{m}$  gap between the wires.

The X-ray patterns in Figure 7 show the magnified images of the 13th pair of Pt wires. The X-ray patterns with a threefold magnification were obtained for the orientation of the Si wafer  $\theta_o = 0.05^\circ$  and

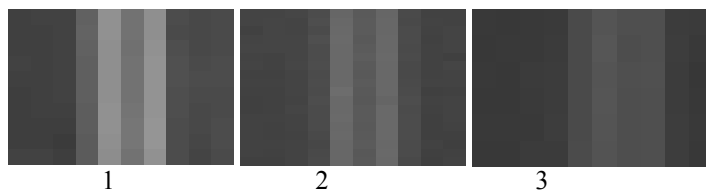


**Figure 7.** The X-ray patterns of 13<sup>th</sup> pair of wires obtained at the angular positions of the pair  $\theta = -0.1^\circ$ ;  $-0.84^\circ$  and  $-1.54^\circ$  relative to the electron beam, patterns 1–3, respectively.

the angular positions of of the pair  $\theta = -1.45^\circ$ ;  $-0.89^\circ$  and  $-0.15^\circ$  relative to the direction of the electron beam, photographs 1–3, respectively. The calculated value of the source size  $S_H$  that corresponds to the above mentioned angular positions  $\theta$  of the 13th pair in the radiation cone are  $S_H = 57$ , 108 and 147  $\mu\text{m}$ , since  $\theta_H = -0.1^\circ$ ;  $-0.84^\circ$  and  $-1.4^\circ$ , respectively. These images show that photograph 1 demonstrates the best resolution of the 13th wire pair of the *IQI* device, and it corresponds to the minimum  $S_H$ . As can be seen, displacement of the object from the cone axis decreases the image quality of the 13th pair due to increased  $S_H$ . The images of wires unite into a single image.

### 6. Conclusion

The experiments have shown that under interaction of 18 MeV electrons of the internal beam of the B-18 betatron with narrow target, the change of the angle of the electrons incident on the target in the range of grazing angles greatly affects the form of angular distribution of the generated radiation. Significant changes of angular distributions are observed when the direction of the target plane is close to the electron beam direction. When orienting the target along the direction of the electron beam, radiation is emitted into two overlapping cones. This effect increases the width of the angular distribution of bremsstrahlung because these radiation components are located on both sides from the direction of the target plane.

The study shows also for the first time the possibility to successfully generate radiation in a narrow target which width can be a couple of hundred times smaller than the diameter of the betatron electron beam, and to use this radiation for obtaining the magnified high resolution images of microstructures with participation of a phase-contrast effect in formation of the images. For the target extended along the electron beam, the decreased contrast of the microstructures details can be caused by its position in the radiation cone due to the increased effective size of the source, the value of which depends on the direction of emission of radiation.

In our case, the radiation spectrum of the betatron generated in narrow internal targets extends from several keV to 18 MeV. For light targets, the images of non-thick objects are formed by emitting a soft part of the radiation spectrum. With heavy targets, the radiation spectrum is dominated by hard radiation due to strong absorption of radiation of the soft part of the spectrum in the target. The radiation generated in such targets is applicable for obtaining images of thick objects from heavy materials.

### Acknowledgments

This work is supported by the Russian Science Foundation, project № 17-19-01217.

### References

- [1] Pushin V S, Chakhlov V L 1997 *RF Patent* № 2072643
- [2] Kasyanov V A, Mikhalechuk A A, Pushin V S, Romanov V V, Safronov A S, Chakhlov V L, Matte M M 1998 Formation of a small-size focal spot of bremsstrahlung in the betatron. *Devices and experimental procedure* **1** 41
- [3] Yamada H 2003 *Nucl. Instrum. Meth. B* **199** 509
- [4] Rychkov M M, Kaplin V V, Sukharnikov K, Vaskovskii I K 2016 *JETP Lett* **103/11** 723
- [5] *Website of the Computerised Information Technology Ltd*: [http://www.cituk-online.com/acatalog/Section\\_NDT\\_Digital\\_Radiography\\_Calibration\\_Devices.html](http://www.cituk-online.com/acatalog/Section_NDT_Digital_Radiography_Calibration_Devices.html)
- [6] Bavendiek K, Ewert U, Riedo A et al 2012 *Proceedings of the 18<sup>th</sup> world conference on nondestructive testing* [http://www.ndt.net/article/wcndt2012/papers/346\\_wcndtfinal00346.pdf](http://www.ndt.net/article/wcndt2012/papers/346_wcndtfinal00346.pdf)
- [7] Wilkins S V, Gureyev TE, Gao D, Pogany A, Stevenson AW (1996) Phase-contrast imaging using polychromatic hard x-rays. *Nature* **384** 335